ning by Saari and Shorthill showed "hot spots," many of which coincided with transient event sites. Many of the locations of Middlehurst and Kuiper were the sites of repeat events, leading to the conclusion that these were possibly volcanic in nature.

If water were formed on the lunar surface in the past through volcanic activity, remnants of frozen H_2O could be expected to survive in the polar regions and in crater rims, protected by meters of fine (15-μm) lunar regolith from the high-vacuum, high-escape velocity, and the long, hot lunar day.

More lunar volcanic resources may possibly be present on the highlands than heretofore believed, a belief based in part on remote sensing of the lunar limb and farside by the Galileo spacecraft in 1990. The probe discovered probable volcanic "cryptomare" provinces on the highlands. Highland volcanism enhances the probability of endogenic water resources on the floors of shadowed polar craters in addition to possible cometary ice input. Modification of Strategic Defense Initiative weaponry for use as orbiting cislunar remote sensors could be useful in detecting ice or ice clathrate within polar craters especially in the vicinity of lunar transient sites. Focused neutron beams from a linear accelerator in polar orbit could be directed onto the floors of eternally shadowed crater floors to detect possible water ice by the 2.22-meV gamma backscatter of hydrogen. Prior to renewed manned exploration of the Moon, many modified SDI systems could be used in active remote sensing exploration for both volcanic and impact-derived volatiles in lunar shadow.

The exploration system seeks to find a surprisingly small amount of water ice. The H_2O would be used for massive cargo propulsion, life support, and material processing. Direct use of the water as propellant in nuclear thermal steam rockets provides nearly the optimum ratio of payload mass per tanker ship mass for lunar ascent and escape missions. The simplicity is of very high practical value to lunar operations. Converting the water into cryofuels provides the most resource-efficient propulsion. To supply 10,000 tons of propellant or rocket fuel to lunar escape would require finding a block of permafrost less than 35 m across. This 10 ktons of fuel is about as much as has been launched during the entire history of space. It would provide the fuel to take 50 payloads of 100 tons each from the lunar surface to an Earth orbit, or to take 25 payloads of 100 tons each to the Moon from low Earth orbit. To deliver 10,000 tons of lunar mass to each of 100 solar power stations of multigigawatt capacity would require finding a mere 160-cubic-meter block of ice.

Prepared for the U.S. Department of Energy Assistant Secretary for Conservation and Renewable Energy under DOE Idaho Field Office Contract OE-AC07-76ID01570.

LUNAR MAGNETIC FIELDS: IMPLICATIONS FOR RESOURCE UTILIZATION.

L. L. Hood, Lunar and Planetary Laboratory, University of Arizona, Tucson AZ 85721, USA.

It is well known that solar-wind-implanted hydrogen and helium-3 in lunar soils are potentially usable resources for future manned activities. Hydrogen applications include manufacture of propulsion fuel and combination with oxygen (extracted from minerals such as ilmenite) to produce water. More speculatively, helium-3 may ultimately be returned to Earth as a fuel for future terrestrial fusion reactors. For economical mining of these implanted gases, it is desirable that relative concentrations exceed that of typical soils (e.g., [1]). It has previously been noted that the monthly variation of solar wind flux on the surface due to lunar immersion in the geomagnetic tail may have measurable consequences for resource utilization [2]. In this paper, it is pointed out that, for a constant external flux, locally strong lunar crustal magnetic fields will exert the dominant influence on solar wind volatile implantation rates. In particular, the strongest lunar crustal magnetic fields will both deflect and focus incident ions in local regions leading to local enhancements of the incident ion flux. Thus, the most economical sites for extraction of solar-wind-implanted volatiles may be within or adjacent to strong crustal magnetic fields. In addition, solar wind ion deflection by crustal magnetic fields must be considered in evaluating the issue of whether remnant cometary ice or water-bearing minerals have survived in permanently shadowed regions near the lunar poles [3]. This is because sputter erosion of water ice by solar wind ions has been suggested to be an important ice loss mechanism within permanently shadowed regions [4]. Thus, permanently shadowed regions that are also shielded from the solar wind by locally strong crustal fields could be the most promising locations for the survival of cometary ice.

Although the largest directly measured surface magnetic field was 327 nT at the Apollo 16 site [5], it is likely that much larger surface fields exist elsewhere in regions of strong magnetic anomalies detected from orbit. Modeling of the latter suggests surface fields as large as several thousand nT (several hundredths of a gauss) in restricted regions. Direct surface measurements of incident solar wind ions were obtained at the Apollo 12 and 15 landing sites where surface field amplitudes were only ~38 and ~3 nT respectively. Nevertheless, at the Apollo 12 site, incident ions were observed to be decelerated by as much as 70 km/s and to be deflected in direction by ≤10° [6]. We have previously calculated the deflection of solar wind ions by simulated lunar crustal magnetic fields for the purpose of investigating the origin of swirl-like albedo markings that are associated with many of the strongest lunar magnetic anomalies [7]. It was found that significant deflections do occur and that local plasma voids are produced at the lunar surface.

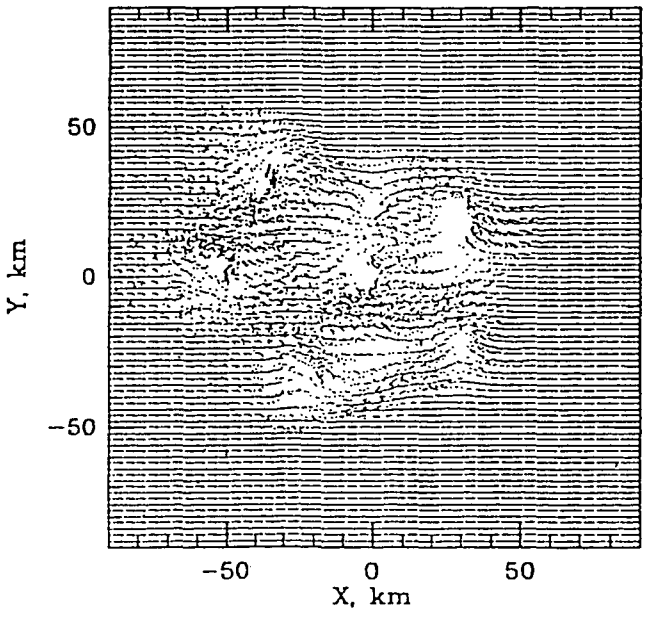

Fig. 1.

In this paper, additional numerical simulations are employed to show that solar wind ion deflection by strong lunar magnetic anomalies can produce local increases in the implantation rate of solar wind gases such as hydrogen. This may increase the resource potential of these volatiles. An example of the surface "shot pattern" produced in one such simulation is shown in the figure. The calculation includes a first-order accounting for the compression (and consequent local amplification) of crustal magnetic fields by the incident solar wind. The net effect is a slight increase in the deflection of ions as compared to that which would occur in the absence of field compression. As a nominal model of a large-amplitude, complex magnetic anomaly source region, we consider a magnetization source distribution represented by a series of dipoles with locations, orientations, and magnetic moments similar to those tabulated in [7]. The resulting magnetic anomaly fields are comparable to those measured over large anomaly sources with the Apollo subsatellite magnetometers. Surface fields are a maximum of ~3000 nT, or about 1 order of magnitude larger than that measured at the Apollo 16 landing site.

Additional simulations indicate that if water ice exists in permanently shadowed regions of the lunar poles together with locally strong magnetic fields, these fields would be capable of preventing sputter erosion losses by interplanetary and magnetospheric ion fluxes. In particular, model simulations indicate that the ability of magnetic anomalies to shield the surface from incident ions increases with the angle of incidence and, hence, for most particle sources, with selenographic latitude.

The possibility that relatively strong anomalies are capable of providing significant protection of humans and materials against major solar flare particle events has also been examined and found to be unlikely.

References: [1] Haskin L. A. (1985) In *Lunar Bases and Space Activities of the 21st Century* (W. Mendell, ed.), 435–444, LPI, Houston. [2] Swindle T. D. et al. (1991) paper presented at the DPS meeting, Palo Alto, CA. [3] Arnold J. R. (1979) *JGR*, *84*, 5659–5668; Arnold J. R. (1987) *LPSC XVIII*, 29–30. [4] Lanzerotti L. J. et al. (1981) *JGR*, *86*, 3949–3950. [5] Dyal P. et al. (1974) *Rev. Geophys. Space Phys.*, *12*, 568–591. [6] Clay D. E. et al. (1975) *JGR*, *80*, 1751–1760. [7] Hood L. L. and Williams C. R. (1989) *Proc. LPSC 19th*, 99–113.

MAPPING THE MOON IN SOFT X-RAYS: PROMISES AND CHALLENGES.

R. M. Housley, Rockwell International Sciences Center, P.O. Box 1085, Thousand Oaks CA 91360, USA.

Recent ROSAT images reported by Schmitt et al. [1] show that the sunlit part of the Moon is a significant source of very soft X-rays. Stimulated by these observations, Edwards et al. [2] have made an analysis of the response of the Moon to the solar soft X-ray and EUV spectrum. They argue that much of the observed emission is in the form of discrete fluorescence lines in the energy range 25 to 100 eV, and that these lines are generally much stronger than the adjacent directly scattered solar background. On this basis they suggest that soft X-ray fluorescence can be used to remotely obtain high-precision elemental maps of the lunar surface. Edwards et al. have continued to develop this idea and have suggested a system using soft X-ray telescopes in lunar orbit, which could also obtain very good spatial resolution (personal communication, 1992). This combination could be extremely valuable in furthering our understanding of lunar chemistry and potential resource distributions.

The fluorescence X-rays considered by Edwards et al. [2] all necessarily involve transitions between the valence band and very shallow core vacancies. Their energies, structures, and overall widths hence reflect the characteristics of the host matrices, and vary with valence state and coordination. In determining line structures, valence electrons derived from the fluorescing atoms' atomic states generally contribute most heavily and their weighting depends on dipole selection rules. Thus even two elements in the same compound are expected to have significantly different line shapes.

In light of the above it is clear that lunar mapping missions could best be planned using actual soft X-ray fluorescence spectra of representative lunar regolith samples, and the component minerals and glasses that make them up. Since such data are not currently available we here use our published XPS data on lunar samples [3] along with unpublished data on minerals to estimate most probable X-ray energies and allowed ranges. This is possible since both the core levels and the valence band levels are seen in the XPS data. The results are presented in Table 1.

TABLE 1. X-ray fluorescence energies and linewidths.

Element	Fluorescence Transition	Predicted Energy (eV)	Allowed Range (eV)	Reference	Samples Used
Na	$L_{23}V$	22	±6	u	Labradorite
Mg	$L_{23}V$	42	±4	u	Forsterite
		42	±7	3	Synthetic lunar glass
		42	±7	3	Lunar regolith 10084
Al	$L_{23}V$	66	±6	u	Labradorite
		67	±6	u	Synthetic lunar glass
		67	±6	u	Lunar regolith 10084
Si	$L_{23}V$	94	±6	u	Labradorite
		95	±4	u	Forsterite
		94	±7	u	Synthetic lunar glass
		96	±7	u	Lunar regolith 10084
S	$L_{23}V$	156	±8	u	FeS
		154	±7	u	ZnS
Ca	$M_{23}V$	18	±6	u	Labradorite
		19	±7	3	Synthetic lunar glass
		18	±7	3	Lunar regolith 10084
Ti	$M_{23}V$	32	±7	u	Ilmenite
		31	±7	3	Synthetic lunar glass
		30	±7	3	Lunar regolith 10084
Fe	$M_{23}V$	49	±7	u	Ilmenite
		49	±7	3	Synthetic lunar glass
		49	±7	3	Lunar regolith 10084
Zn	$M_{23}V$	80	±6	u	ZnS
		80	±6	u	ZnO